EnvironmentAsia
The international journal by the Thai Society of Higher Education Institutes on Environment

EnvironmentAsia 11(3) (2018) 27-44
DOI 10.14456/ea.2017.36
ISSN 1906-1714; ONLINE ISSN: 2586-8861

Remote Sensing and GIS-based River Bank Accretion/Erosion Assessment in the Confluence of Thao-Da-Lo Rivers, North East of Vietnam

Tuyen Danh Vu[1] and Thanh Tien Nguyen[2*]

[1] *Department of Training, Ha Noi University of Natural Resources and Environment, Ha Noi 100000, Viet Nam.*
[2] *Faculty of Surveying, Mapping and Geographic Information, Ha Noi University of Natural Resources and Environment, Ha Noi 100000, Viet Nam.*

* Corresponding author: tdgis_ntthanh@163.com
Received: February 2, 2018; Accepted: June 12, 2018

Abstract

River bank accretion/erosion is the most important geomorphological processes in natural process attracting a great deal of attention from river engineering scientist. In this study, river bank accretion/erosion assessment in the confluence of Thao-Da-Lo rivers in the period of 1986-2017 is presented based on the combination of histogram thresholding and band ratio techniques. Landsat 5 TM and 8 OLI imageries were first used of river bank extraction, GIS was then employed to assess river bank changes and accretion/erosion. It was found that, Thao-Da-Lo river banks have changed complexly, especially on the left bank. Accretion and erosion occurred frequently on both sides of the river, mainly occurred in the left bank of the confluence area such as Tan Duc (Ba Vi district), Minh Nong and Ben Got (Viet Tri city). Almost no erosions were found in the right bank (Phong Van, Co Do, Phu Cuong, Tan Hong, Chau Son and Phu Phuong) in this period. The study showed the effective use of remote sensing and GIS in river bank accretion/erosion assessment.

Keywords: River bank; Accretion/Erosion assessment; Thao-Da-Lo river; Landsat imageries

1. Introduction

River bank changes such as bank erosion, down-cutting and bank accretion, are natural processes for an alluvial river (Kummu *et al.,* 2008). Developments like sand mining, infrastructure building on the riverbank, artificial cutoffs, bank revetment, construction of reservoirs and land use alterations have caused bank river accretion/erosion (Li *et al.,* 2007; Rinaldi, 2003). Bank river changes caused by these human activities may result in various environmental and social-economic consequences such as loss of riparian land and infrastructure, flood hazard and the alteration of aquatic and riparian ecosystems (Kummu *et al.,* 2008). It is therefore, river bank accretion/erosion assessment is of great importance for environmental management.

River bank have been monitored conventionally by ground survey techniques from 1807 to 1927 (Alesheikh *et al.,* 2007). Later, aerial photographs were used for river bank extraction, especially for costal mapping even at a regional scale (Lillesand *et al.,* 2014). However, these techniques are expensive and time-consuming and require trained staff (Ghosh *et al.,* 2015). Recently, remote sensing and geographical information systems (GIS) have been widely used to complement the conventional method for monitoring river bank change (Ryu *et al.,* 2002; Yamano *et al.,* 2006), especially since Landsat and other remote sensing satellites provide digital imagery in infrared spectral bands where the land-water interface is well defined (Alesheikh *et al.,* 2007). It is therefore, several image processing techniques have been introduced in recent decades for the extraction of water features from satellite data. Single-band methods to extract water features by using a selected threshold value (Du *et al.,* 2012). Multi-band methods were proposed for improved surface water extraction by combining different reflective bands (Du *et al.,* 2012), for instance, the Normalized Difference Water Index (NDWI) was developed for the extraction of water features from Landsat imagery (McFeeters, 1996), a modified NDWI (MNDWI) was developed in which the middle infrared (MIR) band was replaced with the near infrared (NIR) band (Xu, 2006). Classification techniques adopted to extract surface water are normally more accurate compared with single-band methods (Du *et al.,* 2012). Based on the advantages and drawbacks of the above methods, Alesheikh *et al.* (2007) developed a new procedure for coastline change detection using remote sensing based on a combination of histogram thresholding and band ratio techniques. It was proven that, histogram thresholding is inadequate in depicting the real changes especially in marsh area, as any threshold value will be exact only on some area. For Landsat-5 TM images, using the band ratio between near infrared band (0.76 – 0.90 μm) and green band (0.52 – 0.60 μm), and also, between Shortwave Infrared (SWIR) 1 (1.55-1.75 μm) and green band can result in water-land discrimination (Alesheikh *et al.* 2007). It is therefore, the combination of histogram thresholding and band ratio techniques are applied to assess river bank accretion/erosion in this study.

Recent damages caused by river bank erosion in the confluence of Thao- Da- Lo rivers have been frequently reported. For example, due to the impact of the tenth typhoon and long lasting of heavy rains on Sept. 2017 has caused bank erosion, river bank breaking in the

commune of Song Lo, Viet Tri city. River bank erosion happened on two serious points with the length along the river nearly 400 meters; the widest erosion point was about 30m, a total of 8,000 m2 of crop area was flowed into the river (QĐND, 2017). The impact of bank erosion on humans and poverty is a serious problem in this area. It is therefore, in this study, the river bank accretion/erosion in the confluence of Thao-Da-Lo rivers in the period 1986 - 2017 were investigated using remote sensing and GIS.

2. Study area and data used

2.1 Study area

Thao-Da-Lo confluence is located in the districts of Lam Thao, Tam Nong, Viet Tri city (the capital of Phu Tho province) and Ba Vi district (Ha Noi) - north east of Vietnam (Figure 1.). It's length is over 30 km. The Red River section at the confluence is an inverted U shaped. The Red River flood season at confluence usually starts from June to October with total water volume accounting for 70-80% of total annual flow, especially floods often occur in July and August. The flow regime of the confluence zone depends very tightly on the flow regime of three Thao, Da and lo tributary rivers, the hydrological, hydraulic regimes of the Red river in this section are therefore very complex, leading the changes in the confluence of the river bed.

Tectono-structural characteristics: the Thao, Da and Lo confluence is influenced by the faults of the SE-NW fault system, including the Red river, Chay river, the NE-NW fault system, the sub-meridional and eccentric tectonic fault systems. The SE-NW fault system forms the Hoa Binh-Trung Ha depressed rift, which controls the flow of the Da river from the section of Hoa Binh to the confluence of Thao river. The Red River fault has the north-southern compression

Figure 1. Location of the confluence of Thao-Da-Lo rives.

creating the rift zones at the intersections with the corresponding NE-NW faults such as the Thao-Da confluence (Figure 1). It is the combined effects of the activities of the above fault systems that form the incomplete bending river morphology in the confluence. It is therefore, the river bed always tends to develop to the north (side of the rift) (Xuan, 2012).

River morphological characteristics: This river section is an inverted U-shaped bend. It's mainstream usually gets close to the bank causing frequent bank erosion at the crest areas (the concave side of the bend) such as at Thuy Van, Tan Duc and Minh Nong communes (Xuan, 2012).

Characteristics of sediment and physical properties of rocks of river banks: rocks forming river banks in this area are mainly composed of Holocene-aged easily breakable and friable sedimentary rocks of belonging to alluvial plains including: clay, sand, fine sand, organic clay mud and the top layer of alluvial soil; the lower depth, the rate of sand increases; and mainly discrete-state fine sand at an average depth of about less than 10m. This sand layer is easily subjected to runoff drift, causing bank erosion. The analysis results of river bank physical properties of confluence showed that the non-erosion velocity of the granule constituents is less than 1.5 m/s. In the case that the velocity of the Red River flow is quite large (the maximum flow velocity measured at Thuy Van commune was about 1.82 m/s at 9/2002), riverbank erosion will occur on many areas (Xuan, 2012).

Hydrological characteristics: flows from Thao, Da and Lo rivers interact to each other forming very complex and spiral flows in the confluence zone. When the whirlpools press to river banks causing bank erosion. The erosions of the river banks in the confluence are complex and no clear rules due to the location and the destructive intensity of the continuously changed turbulent flows of each tributary flow when they flow into the confluence zone. The Red River has a very complex hydrological regime with high flow rates. In addition, floods are frequent during the flood season, but often the velocities of tributary inflows are different. The site of erosion and river bank destruction intensity depend heavily on the contribution of flood flows of the three tributaries (Ngo *et al.,* 2005).

2.2 Data used

Table 1. Data used in the study

Data type	Satellite-sensor	Date of acquisition	Path/row	Spatial resolution/Scale
Remote sensing images	Landsat-5 TM	1986-07-01	127/045	30 m
	Landsat-5 TM	1992-08-18	127/045	30 m
	Landsat-5 TM	1998-07-18	127/045	30 m
	Landsat-5 TM	2002-07-13	127/045	30 m
	Landsat-5 TM	2008-07-29	127/045	30 m
	Landsat-5 TM	2010-06-17	127/045	30 m
	Landsat-8 OLI	2017-06-04	127/045	30 m
Boundary map		2016		1/50,000

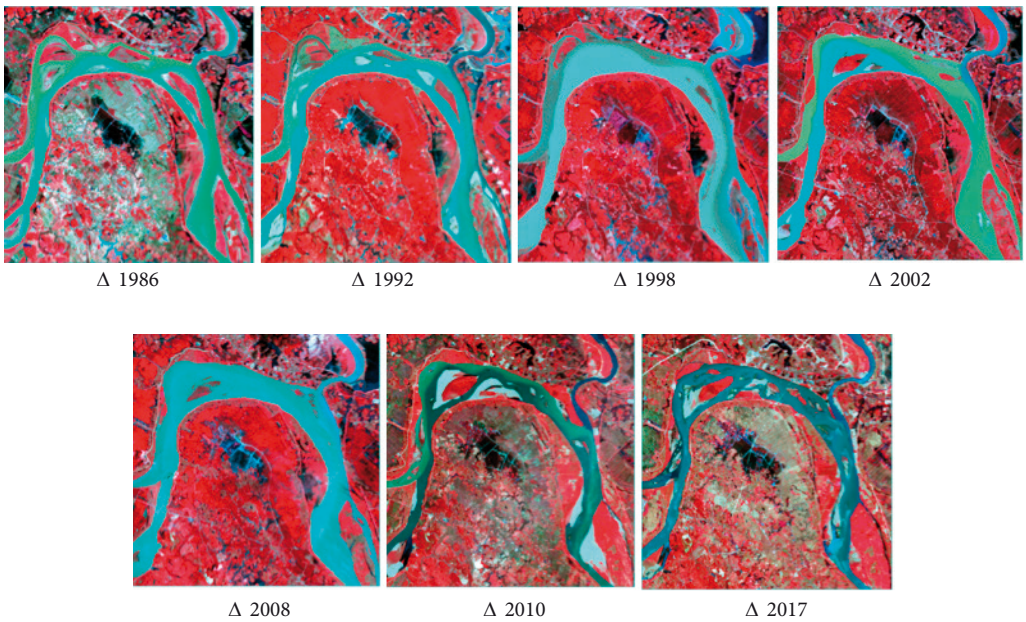

Figure 2. False colour composite Landsat images acquired in the confluence of Thao-Da-Lo rives.

In this study, daytime cloud-free Landsat-5 TM and -8 OLI images with 30-m spatial resolution were collected (Figure 2 and Tab. 1). All the Landsat TM/OLI datasets were the standard terrain correction (L1T) products, downloaded from the United States Geological Survey website (USGS), which provides systematic radiometric and geometric accuracy estimates by incorporating ground control points (GCPs) from the global land survey of 2000 (GLS2000) and employing a digital elevation model (DEM) for topographic accuracy. DEM sources include the Shuttle Radar Topography Mission (SRTM), the National Elevation Dataset (NED), Canadian Digital Elevation Data (CDED), Digital Terrain Elevation Data (DTED), and GTOPO 30 (a global DEM from the USGS). The Universal Transverse Mercator (UTM) projection with zone 48 with datum and ellipsoid of World geodetic system (WGS) 84 are used in all the Landsat data. In addition, a map boundary and accretion/erosion reports are also used in this study for the assessment.

3. Methods

The flowchart of the methodology used for this study is given in Figure 3.

3.1 Image pre-processing

a. Conversion to at-sensor spectral radiance

Conversion to at-sensor spectral radiance is the first step in converting image data from multiple sensors and platforms into a physically meaningful common radiometric scale. In this process, pixel values from raw unprocessed image data are converted to units of absolute spectral radiance using inflight sensor calibration parameters (Chander *et al.,* 2003). The absolute spectral radiance values are then scaled to 8-bit (TM, Q_{cal_max} = 255) and 16-bit (OLI, Q_{cal_max}

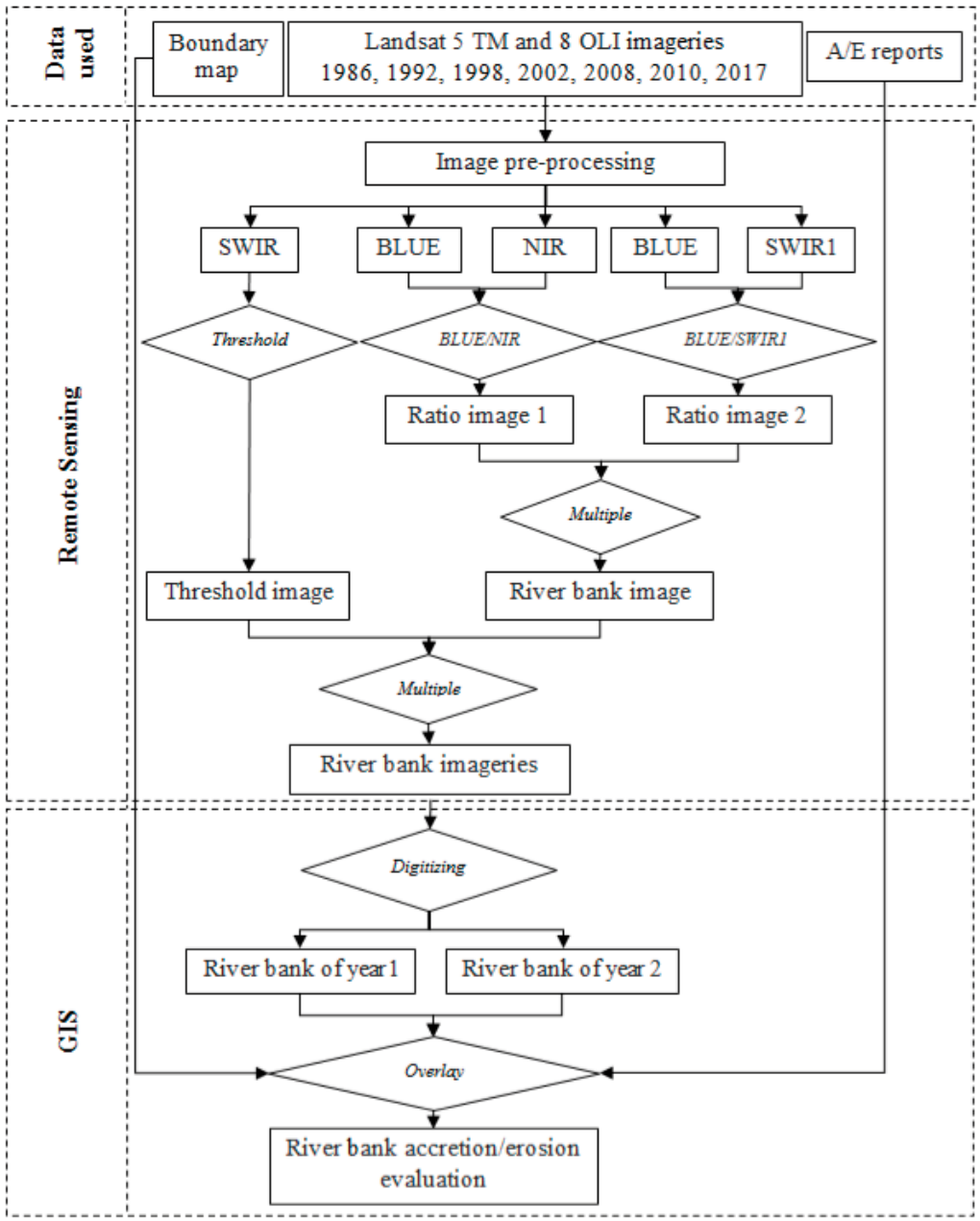

Figure 3. Flow chart of bank river accretion/erosion assessment using remote sensing and GIS.

= 32767). The following equation is used to perform the Q_{cal}-to-L_λ conversion for Landsat TM (Chander *et al.*, 2009):

$$L_\lambda = \left(\frac{Lmax_\lambda - Lmin_\lambda}{Q_{cal\_max} - Q_{cal\_min}}\right) \times (Q_{cal} - Q_{cal\_min}) + Lmin_\lambda \quad (1)$$

where: L_λ is spectral radiance at the sensor's aperture [$W/m^2.sr.\mu m$]; Q_{cal} is quantized calibrated pixel values (DN values); Q_{cal_min} and Q_{cal_max} are minimum quantized calibrated pixel values corresponding to $Lmin_\lambda$ and $Lmin_\lambda$ respectively; $Lmin_\lambda$ and $Lmax_\lambda$ are spectral

at-sensor radiance, scaled to Q_{cal_min} and Q_{cal_max} respectively [W/m^2.sr.μm].

For Landsat 8 OLI, Eq. (2) is used to perform the conversion (Mishra *et al.,* 2014):

$$L_\lambda = M_L.Q_{cal} + A_L \quad (2)$$

where: M_L, A_L are respectively band-specific multiplicative rescaling factor and band-specific additive rescaling factor from the metadata; Q_{cal} is quantized calibrated pixel values.

b. Atmospheric correction

To correct atmospheric effects, different strategies have been developed, such as image-based atmospheric correction methods including Dark Object Subtraction (DOS) (Wang *et al.,* 2009), Cosine of the sun zenith angle COST (Canadell *et al.,* 2008), and QUick Atmospheric Correction (QUAC) (Houghton, 2005); the Simplified Method for Atmospheric Correction (SMAC) (Zhu *et al.,* 2015); the Empirical Line Calibration (ELC) (Fournier *et al.,* 2003); other more complex approaches model based on an accurate radiative transfer code (RTC) to correct the atmospheric effects, such as the MODerate resolution atmospheric TRANsmission (MODTRAN) (Hese *et al.,* 2005; Parresol, 1999), the ATmospheric CORrection (ATCOR) (Hadjimitsis *et al.,* 2010; Heo *et al.,* 2000), the Second Simulation of a Satellite Signal in the Solar Spectrum (6S) (Fraser *et al.,* 1977; Kawata *et al.,* 1990), and the Fast Line-of-sight Atmospheric Analysis of Spectral Hypercubes (FLAASH) (Fuchs *et al.,* 2009) models. Among these models, FLAASH has been widely applied by many studies (Afify *et al.,* 2017; Govil *et al.,* 2018; Meehan, 2016; Onojeghuo *et al.,* 2018).

FLAASH starts from a standard equation for spectral radiance at a sensor pixel, L, that applies to the solar wavelength range (thermal emission is neglected) and flat, Lambertian materials or their equivalents. The spectral radiance is calculated using Eq. (3) (Adler-Golden *et al.,* 1998; Adler-Golden *et al.,* 1999):

$$L^* = \left(\frac{A\rho}{1-\rho_e S}\right) + \left(\frac{B\rho_e}{1-\rho_e S}\right) + L_a^* \quad (3)$$

where: ρ is the pixel surface reflectance; ρ_e is an average surface reflectance for the pixel and a surrounding region; S is the spherical albedo of the atmosphere; L_a^* is the radiance back scattered by the atmosphere; A and B are coefficients that depend on atmospheric and geometric conditions but not on the surface.

The values of A, B, S and L_a^* are determined from MODTRAN4 calculations that use the viewing and solar angles and the mean surface elevation of the measurement, and they assume a certain model atmosphere, aerosol type, and visible range. After the water retrieval is performed, the spatially averaged reflectance ρ_e is estimated using Eq. (4) (Adler-Golden *et al.,* 1998; Adler-Golden *et al.,* 1999):

$$L_e = \left(\frac{(A+B)\,\rho_e}{1-\rho_e S}\right) + L_a^* \quad (4)$$

The FLAASH model includes a method for retrieving an estimated aerosol/haze amount from selected dark land pixels in the scene. The method is based on observations by (Kaufman *et al.,* 1997) of a nearly fixed ratio between the reflectances for such pixels at 660 nm and 2100 nm.

3.2 River bank extraction

River bank can be extracted by histogram thresholding on one of the infrared bands, since the reflectance of water is nearly equal to zero in reflective infrared bands, and reflectance of absolute majority of land covers is greater than water (Alesheikh *et al.,* 2007). *(Kelley et al., 1998)* recommended, mid-infrared band (band 5 of Landsat-5 TM and band 6 of Landsat 8 OLI) is the best for extracting the land-water interface due to the high degree of absorption of mid-infrared energy by water and strong reflectance of mid-infrared by vegetation and natural features in this range. In this study, the histograms of mid-infrared bands of Landsat images display a sharp double peaked curve. Threshold values were selected to find transition zones between land and water resides between the peaks. Threshold images were then converted to binary-threshold images. (Alesheikh *et al.,* 2007) showed that, any threshold value will be exact on some area, not all. Band ratio for the direct separation of water and land was then used to complement this drawback. Band ratio between BLUE band and SWIR1 band is expressed by Eq. (5):

$$R_{B/S}=\left(\frac{R_{BLUE}}{R_{SWIR1}}\right)\begin{cases}\text{If } R_{B/S}>1\text{, then extracted area is water}\\ \text{If } R_{B/S}<1\text{, then extracted area is soil}\end{cases} \quad (5)$$

This law is for the extraction of water and land covered by soil, but not in land with vegetative cover. To solve this difficulty, band ratio between BLUE band and NIR band is then used extract water and land covered by vegetation, and expressed by Eq. (6):

$$R_{B/N}=\frac{R_{BLUE}}{R_{NIR}}\begin{cases}\text{If } R_{B/N}>1\text{, then extracted area is water}\\ \text{If } R_{B/N}<1\text{, then extracted area is vegetation}\end{cases} \quad (6)$$

Both of ratio images were then converted to binary images with the values of 0 represented for land and the value of 1 represented for water. River bank image results in multiplying binary-threshold images and binary-ratio images.

3.3 River bank river accretion/erosion assessment

To detect the changes along the river bank, river bank images of different years were overlaid and on-screen digitizing of river bank was undertaken to create the river bank layers. Layers were overlain together with boundary map so that the river bank position could be seen at each date. River bank positions were highlighted to infer the accretion/erosion along the river bank, and the river bank changes were visualized and calculated. Accretion/erosion assessment was then carried out in combination with annual reports on accretion/erosion in the confluence of Thao-Da-Lo rivers.

3.4 Data treatment and soft wares used

All of the Landsat images were collected from website of The United States Geological Survey. The work of river bank extraction such as radiometric calibration, atmospheric correction through FLAASH module, subset of study area, threshold images and ratio images was done in ENVI 5.2 software. The digitizing, overlay of boundary and river bank layers and mapping accretion/erosion were carried out in ArcGIS 10.2 software.

4. Results and discussions

Summary results of Thao-Da-Lo river banks accretion/erosion in the period of 1986 - 2017 using Landsat imageries are shown in Figure 4 and Tab. 2.

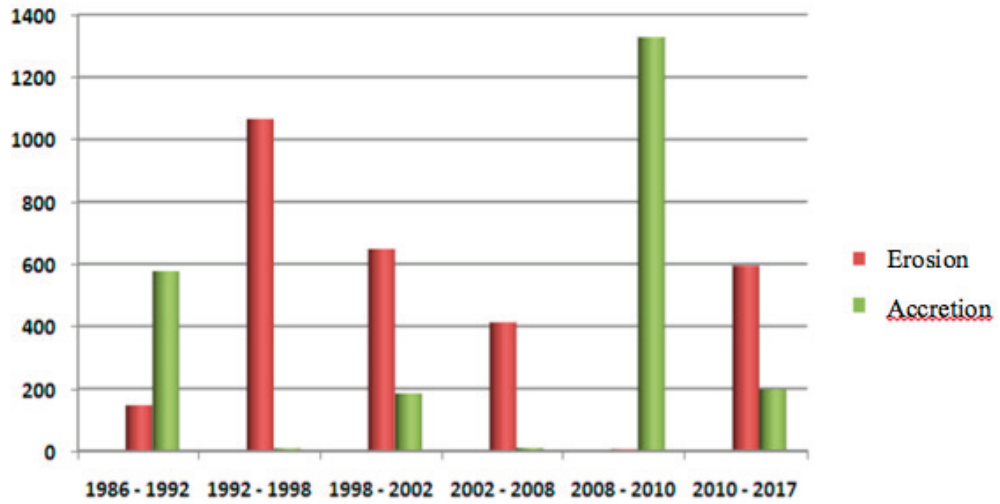

Figure 4. Plot of accretion/erosion in the period of 1986 - 2017.

Table 2. Summary table of accretion/erosion in the period of 1986 - 2017.

Period	Erosion area (hectares)	Accretion area (hectares)
1986 - 1992	146.93	576.45
1992 - 1998	1065.64	7.48
1998 - 2002	648.38	184.35
2002 - 2008	412.33	9.42
2008 - 2010	5.58	1328.06
2010 - 2017	595.1	197.45

4.1 Period of 1986 - 1992

The results of the bank river extraction for the two Landsat TM satellite images acquired in 1986 and 1992 are shown in Figure 5. It can be seen that there were almost no river bank changes in the period of 1986 - 1992. Compared to the river bank extracted in 2010, the accretion zone appeared in some areas of Tan Duc and Phu Son (Ba Vi). The total area of accretion were 576.45 hectares (Figure 4 and Tab. 2). River bank erosion was also found in the areas of Minh Nong (Viet Tri city), Vinh Loi (Lam Thao) and Phu Chau (Ba Vi). The total area of erosion were 149.93 hectares. A total of 280 hectares of natural land were lost in this period compared to 355 hectares (805 households, 3900 people) in 1987, in which 100 hectares of residential land of Tan Duc were lost (Xuan, 2012). Most of the cultivated land along the river was completely eroded. The river bank almost unchanged in the formerly eroded areas such as Ben Got (Viet Tri city), Viet Xuan and Son Dong (Lap Thach). No river bank change was found in the areas of Phong Van, Co Do, Phu Cuong, Tan Hong, Chau Son and Phu Phuong communes (Ba Vi), indicating that there was no accretion or erosion in these areas.

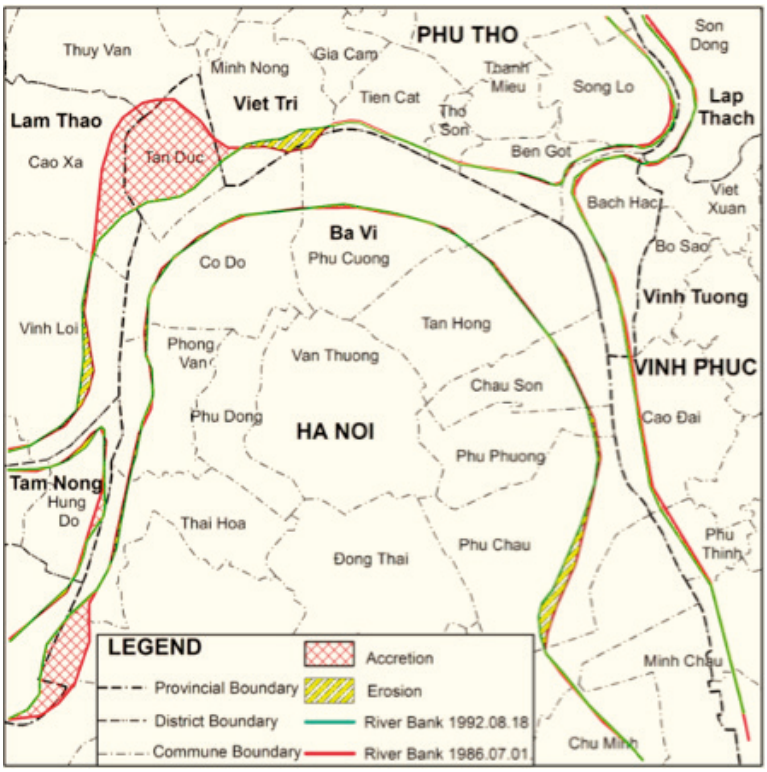

Figure 5. Accretion/erosion in the period of 1986 - 1992.

4.2 Period of 1992 - 1998

The results of bank river extraction from Landsat imageries in 1992 and 1998 in the confluence of the Thao-Da-Lo rivers are shown in Figure 6. It was showed that river bank changes were found in the communes of Song Lo (Viet Tri city) and Son Dong, Viet Xuan (Lap Thach). This showed that serious erosions had occurred in these areas. In addition, erosions were also found in areas such as Tan Duc (Ba Vi), Minh Nong, Phu Chau, Phu Son (Ba Vi) and Phu Thinh (Vinh Tuong). The total area of erosion were 1065.64 hectares comparing with accretion area of 7.48 hectares (Figure 4 and Tab. 2). The results of river bank extraction showed that river bank areas were still very stable in Phong Van, Co Do, Phu Cuong, Tan Hong, Chau Son and Phu Phuong communes (Ba Vi) during this period, indicating no river bank erosions found in these areas. Compared to previous periods, erosions still occurred in the area of Tan Duc and Minh Nong communes, especially seriously eroded areas were detected in the communes of Song Lo (Viet Tri) and Song Dong (Lap Thach). Ming Nong and Tien Cat are the curved top of the river bed. Minh Nong commune (Viet Tri city) had a total of 113.8 ha of land, including 3.8 hectares of residential land, it has lost a total of 91 hectares and 45 households have had to move since 1995 (Xuan, 2012). Tien Cat (Viet Tri City) had a total area of 11 hectares, including 5 hectares of residential land, 2.5 hectares of residential land had lost from 1995 to 2001 and

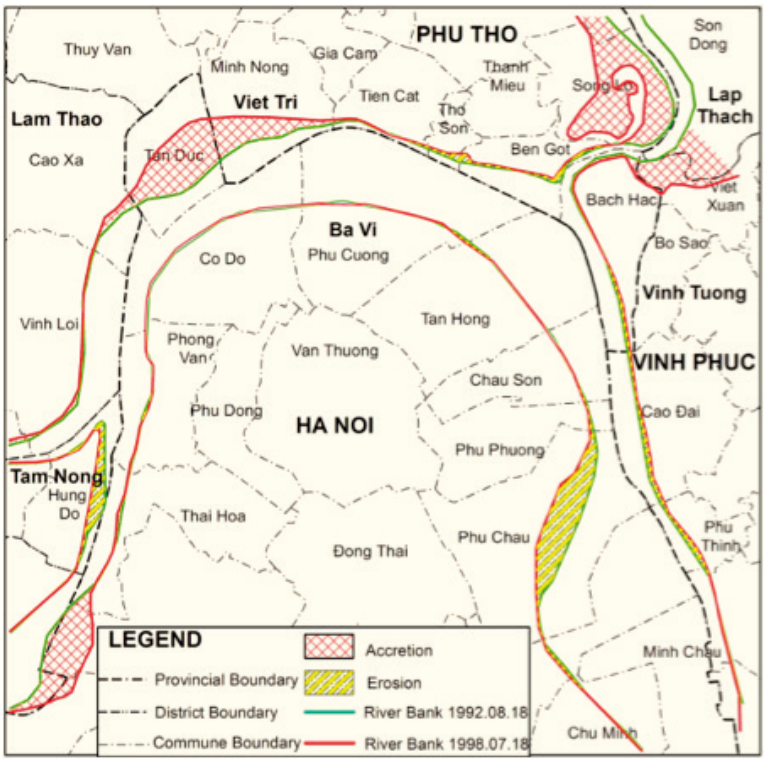

Figure 6. Accretion/erosion in the period of 1992 - 1998.

50 households had to move. The area of Bach Hac (Viet Tri City) had been eroded in almost every year. From 1995 up to now, 8 of 10 hectares of land outside the dyke had been lost and 75 had been removed. There are embankments in some areas, but some flood-prevention dykes is still under threaten in this area. The phenomenon of erosion in this segment has been increasing especially since the Tan Duc embankment existed.

4.3 Period of 1998 - 2002

Bank river accretion/erosion in the period of 1998 - 2002 are shown in Figure 7. It can be seen that serious erosion areas in Song Lo (Viet Tri) and Son Dong, Viet Xuan (Lap Thach) communes last period had been accreted during the year of 1986 and of 1992. However, serious erosions occurred again in Tan Duc (Ba Vi), Cao Xa and Minh Nong communes (Viet Tri city). The total area of erosion were found during this period were 648,38 hectares (Figure 4 and Tab. 2). In particular, erosions occupied most of Tan Duc commune, nearly half of Minh Nong commune and a western part of Cao Xa commune (Lam Thao district). However, compared to the bank river of July 18, 1998, there were some areas of accretion such as Vinh Loi, Cao Xa (Lam Thao), Phu Chau (Ba Vi). During this period, strong erosion area nearly 1km was also found in Co Do (Ba Vi, Ha Noi) of the right river before this period, however, river bank of this area has been temporarily stabilized due to embanked in 1998 and 1999 (Xuan, 2012). The area of Thuy Van was eroded

nearly 50 to 70m in 2001. Particularly, serious erosion were found in the area of Tan Duc in 1987-2001, a commune in the left bank of the Thao River. The number of households having to relocate from 1997 to 2001 was 560 households. Normally, at the beginning of the flood season, or when the Hoa Binh hydropower plant discharges floods, river bank erosion occurs very strongly across the entire river bank lasting 1.5 km. Especially, width of erosion area was from 90 to 100m on June 2001 with the average of 15m per day. The embankment was completed on a stretch of 1.5 km from April 2002 to the end of 2002 (Xuan, 2012). It is therefore, the river bank is now more stable. It is therefore, the right banks belonging to Phong Van, Co Do, Phu Cuong, Tan Hong, Chau Son and Phu Phuong communes (Ba Vi) and the left banks of Tho Son and Tien Cai communes (Viet Tri city) was still very stable, almost no erosion occurred.

4.4 Period of 2002 - 2008

The results of river bank extraction from Landsat 5 TM satellite imageries collected on July 13, 2002 and July 29, 2008 are shown in Fig. 8. It was shown that, at the same time of imaging in July of 2002 and 2008, the river bank mainly changed in the communes of Son Dong (Lap Thach) and Phu Chau (Ba Vi district). Most remain unchanged. This showed that erosions still occurred in Son Dong (Lap Thach district) and Phu Chau (Ba Vi district), especially in many areas of Son Dong commune. The total erosion area of 412,33 hectares were found during this period (Fig.4 and Tab. 2). In many places, there was no change in comparison with the time of July 13th, 2002. This showed that the erosion occurred and occupied most of Tan Duc commune, nearly half of Minh Nong commune and the western part of Cao Xa commune (Lam

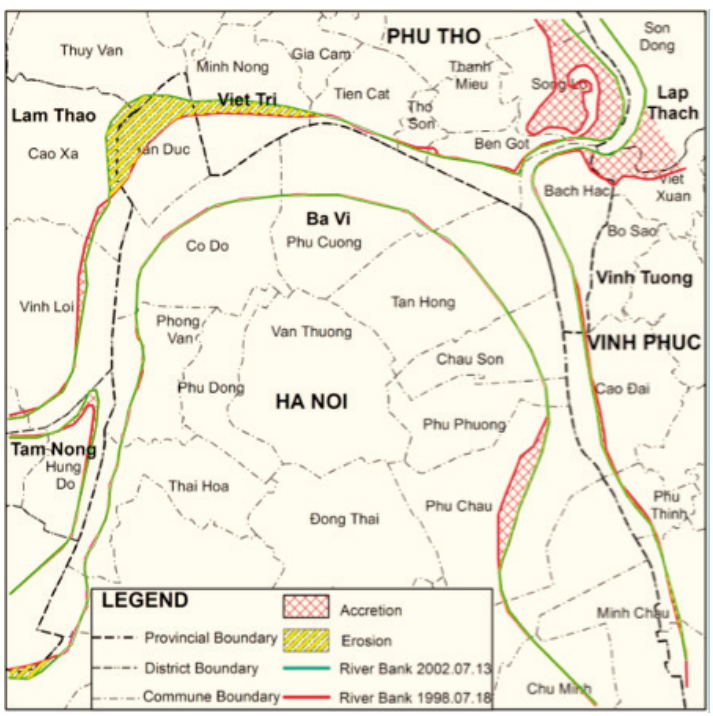

Figure 7. Accretion/erosion in the period of 1998 - 2002

Thao). The stability of river bank was maintained at the right bank of the Phong Van, Co Do, Phu Cuong, Tan Hong, Chau Son and Phu Phuong communes (Ba Vi) and the left bank of the communes of Tho Son and Tien Cat (Viet Tri city), almost no erosions occurred in the period of 2002-2008. In addition, it has been reported, the river bank of Cao Xa (Lam Thao), Thuy Van (Viet Tri) and Tan Duc (Ba Vi) communes had been eroded in this period, especially erosion in 2007 has penetrated up to tens of meters. Erosion approached flood-prevention dyke in the area of Cao Xa, adjacent to Thuy Van. The river bank has been protected by embankment over a length of more than 1km (Xuan, 2012). Strong erosion had occurred on the right river bank of Phong Van commune (Ba Vi, Ha Noi) near the confluence of Thao - Da since 2003. On the bank of the river, small erosions occurred in the area of from Tan Hong commune to Chau Son commune (Ba Vi) at the end of 2005 and the beginning of early 2006. The erosion encroached on river bank to 50m stretching along Van Sa village, Tan Hong area. In addition, there were 185 households in Van Sa village and more than 70 households in La Thien village on the riverside were in danger. This area is now protected by embankments. The river bank erosion of 1.2 km long in the area of Chau Son commune had caused 14 houses, 2 hectares of gardens, yards damaged. The escarpment from 10 to 15m was also found. There are also embankments in some area, but erosion still occurred (Ngo *et al.*, 2005).

Figure 8. Accretion/erosion in the period of 2002 – 2008

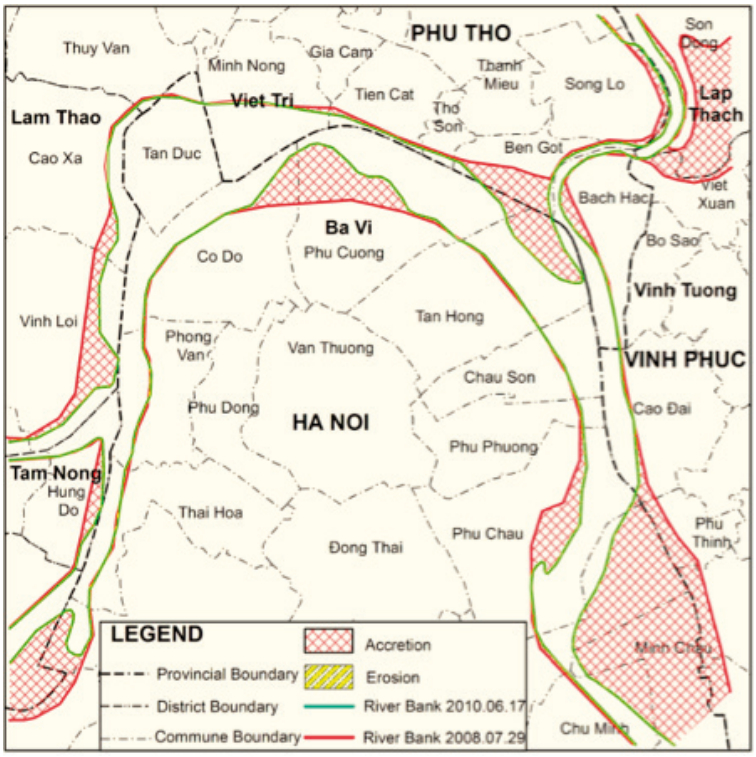

Figure 9. Accretion/erosion in the period of 2008 - 2010.

4.5 Period of 2008 - 2010

The results of accretion/erosion in confluence of Thao - Da - Lo rivers in the period of 2008 and 2010 are shown in Fig. 9. The results showed that there were great changes in river banks, mostly occurred in the area of communes such as Ben Got (Viet Tri), Vinh Loi (Lam Thao), Phu Cuong, Co Do and Phu Chau (Ba Vi) and Minh Chau (Vinh Tuong). It can be recognized that the erosion still occurred in Tan Duc commune (Ba Vi) and Minh Nong (Viet Tri city) with a small area of 5.58 hectares. However, river bank changes were found due to the presence of accretions. The total accretion area of 1328.06 hectares were found during this period (Figure 4 and Tab. 2). River bank accretions were found in the areas of the villages of Ben Got (Viet Tri), Phu Cuong, Co Do and Phu Chau (Ba Vi), Minh Chau (Vinh Tuong) and Vinh Loi (H. Lam Thao). The flow confluence of Thao-Da-Lo confluences was complicated in this period. The results of accretion/erosion extraction for the period 2008-2010 also showed that the right river bank of Ba Vi district (Ha Noi) was mostly unchanged and relatively stable, the river bank changes in Phu Cuong and Co Do communes were found due to accretion in this area.

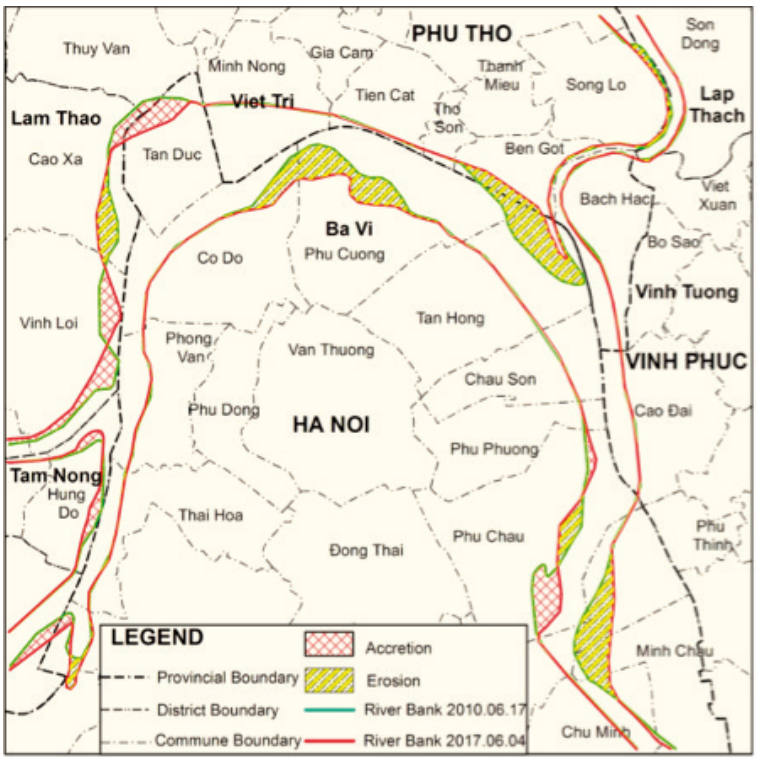

Figure 10. Accretion/erosion in the period of 2010 - 2017.

4.6 Period of 2010 - 2017

The results of accretion/erosion for the period of 2010 and 2017 are shown in Figure 10. It can be seen that, at the same time of imaging in June, but the river banks had a lot of changes. The total erosion area of 595.1 hectares were found compared with accretion area of 197.45 hectares (Figure 4 and Tab. 2). Much changes in river banks occurred in Tan Duc, Ben Got, Cao Xa, Vinh Loi communes of Viet Tri city (Phu Tho province) and Phu Cuong, Phu Chau communes of Ba Vi district (Ha Noi). During this period, bank erosions were also reported on Sept. 2017 breaking in the commune of Song Lo, Viet Tri city. River bank erosion occurred at two serious points with the length along the river nearly 400 meters; the widest erosion point was about 30m, a total of 8,000 m2 of crop area was flowed into the river (QĐND, 2017). Compared with the river banks extracted in 2010, the accretions were found in the areas of Tan Duc (Viet Tri City), Vinh Loi (Lam Thao) and Phu Chau (Ba Vi). The erosions occurred in Phu Cuong, Phu Chau (Ba Vi), Ben Got (Viet Tri City), Cao Xa, Vinh Loi (Lam Thao) and Minh Chau (Vinh Tuong). Stable river banks occurred in the areas of Tien Cat, Tho Son (Viet Tri city), Cao Dai, Bach Hac (Vinh Tuong), Co Do, Phong Van, Thai Hoa (Ba Vi). It can be seen that the river banks of Ba Vi was still relatively stable during this period, the river banks were often changed due to accretions or erosions in the areas such as Tan Duc, Cao Xa and Ben Got.

5. Conclusions

In this study, river bank accretion/erosion assessment in the confluence of Thao-Da-Lo rivers in the period of 1986-2017 was investigated based on GIS and remote sensing techniques. Landsat 5-TM and 8 OLI imageries were used for river bank extraction, GIS was then employed to assess river bank changes and accretion/erosion. The results showed that, Thao-Da-Lo river banks have changed complexly in this period, especially on the left bank. Accretion and erosion were found frequently on both sides of the river bank such as in the areas of Tan Duc (Ba Vi district), Minh Nong and Ben Got (Viet Tri city). Endogenous factors (geology, tectonic structure and activity of tectonic faults) are the main causes of erosion leading to river bank erosion. Exogenous factors such as morphological morphology, hydrological regime, river bank soil texture and human activities also play an important role in promoting this process. The right river banks (Phong Van, Co Do, Phu Cuong, Tan Hong, Chau Son and Phu Phuong) were stable during this period, it is therefore, almost no erosions or accretions were found. It can be concluded from the results of the study that the effectiveness of remote sensing and GIS technology were proved in riverbank accretion and erosion assessment. However, water level data recorded at (near) image acquisition time were not available, and riverbanks in different seasons in a year were not extracted for accretion/erosion assessment in this study. These limitations will be considered in future studies.

References

Adler-Golden SM, Berk A, Bernstein LS, Richtsmeier S, Acharya PK, Matthew MW, Chetwynd JH. FLAASH, a MODTRAN4 atmospheric correction package for hyperspectral data retrievals and simulations. Proc. 7th Ann. JPL Airborne Earth Science Workshop 1998; 97: 9-14.

Adler-Golden SM, Matthew MW, Bernstein LS, Levine RY, Berk A, Richtsmeier SC, Hoke ML. Atmospheric correction for shortwave spectral imagery based on MODTRAN4. In Imaging Spectrometry V, International Society for Optics and Photonics 1999; 3753: 61-70.

Afify NM, Sheta AAS, Arafat SM, Afify AA, El-Beltagy AS. Land-cover classification for east suez canal region using hyperspectral EO-1 data. European Chemical Bulletin 2017; 6:525-530.

Alesheikh AA, Ghorbanali A, Nouri N. Coastline change detection using remote sensing International. Journal of Environmental Science & Technology 2007; 4:61-66.

Canadell JG, Raupach MR. Managing forests for climate change mitigation science 2008; 320: 1456-1457.

Chander G, Markham B. Revised Landsat-5 TM radiometric calibration procedures and postcalibration dynamic ranges. IEEE Transactions on geoscience and remote sensing 2003; 41: 2674-2677.

Chander G, Markham BL, Helder DL. Summary of current radiometric calibration coefficients for Landsat MSS, TM, ETM+, and EO-1 ALI sensors. Remote sensing of environment 2009; 113: 893-903.

Du Z, Linghu B, Ling F, Li W, Tian W, Wang H, Zhang X. Estimating surface water area changes using time-series Landsat data in the Qingjiang River Basin, China. Journal of Applied Remote Sensing 2012; 6: 063609_1-16.

Fournier R, Luther J, Guindon L, Lambert M-C, Piercey D, Hall R, Wulder M. Mapping aboveground tree biomass at the stand level from inventory information: test cases in Newfoundland and Quebec. Canadian Journal of Forest Research 2003; 33: 1846-1863.

Fraser RS, Bahethi OP, Al-Abbas A. The effect of the atmosphere on the classification of satellite observations to identify surface features. Remote Sensing of Environment 1977; 6: 229-249.

Fuchs H, Magdon P, Kleinn C, Flessa H. Estimating aboveground carbon in a catchment of the Siberian forest tundra: Combining satellite imagery and field inventory. Remote Sensing of Environment 2009; 113: 518-531.

Ghosh MK, Kumar L, Roy C Monitoring the coastline change of Hatiya Island in Bangladesh using remote sensing techniques ISPRS Journal of Photogrammetry and Remote sensing 2015; 101:137-144.

Govil H, Gill N, Rajendran S, Santosh M, Kumar S. Identification of new base metal mineralization in Kumaon Himalaya, India, using hyperspectral remote sensing and hydrothermal alteration Ore Geology Reviews 2018; 92: 271-283.

Hadjimitsis DG, Papadavid G, Agapiou A, Themistocleous K, Hadjimitsis MG, Retalis A, Clayton CRI. Atmospheric correction for satellite remotely sensed data intended for agricultural applications: impact on vegetation indices. Natural Hazards and Earth System Sciences 2010; 10: 89-95.

Heo J, FitzHugh TW. A standardized radiometric normalization method for change detection using remotely sensed imagery. Photogrammetric Engineering and Remote Sensing 2000; 66: 173-181.

Hese S, Lucht W, Schmullius C, Barnsley M, Dubayah R, Knorr D, Schröter K. Global biomass mapping for an improved understanding of the CO2 balance—the Earth observation mission Carbon-3D. Remote Sensing of Environment 2005; 94: 94-104.

Houghton R. Aboveground forest biomass and the global carbon balance. Global change biology 2005; 11: 945-958

Kaufman Y, Wald A, Remer L, Gao B, Li R, Flynn L. Remote sensing of aerosol over the continents with the aid of a 2.2 m channel. IEEE Transactions on Geoscience and Remote Sensing. 1997; 35: 1286-1298.

Kawata Y, Ohtani A, Kusaka T, Ueno S. Classification accuracy for the MOS-1 MESSR data before and after the atmospheric correction. IEEE Transactions on Geoscience and Remote Sensing 1990; 28: 755-760.

Kelley JG, Hobgood JS, Bedford KW, Schwab DJ. Generation of three-dimensional lake model forecasts for Lake Erie. Weather and Forecasting 1998; 13: 659-687.

Kummu M, Lu X, Rasphone A, Sarkkula J, Koponen J. Riverbank changes along the Mekong River: remote sensing detection in the Vientiane–Nong Khai area. Quaternary International 2008; 186: 100-112.

Li L, Lu X, Chen Z. River channel change during the last 50 years in the middle Yangtze River, the Jianli reach. Geomorphology 2007; 85: 185-196.

Lillesand T, Kiefer RW, Chipman J. Remote sensing and image interpretation. New Jersey: Wiley and Sons; 2014.

McFeeters SK (1996) The use of the Normalized Difference Water Index (NDWI) in the delineation of open water features. International journal of remote sensing 2014; 17: 1425-1432.

Meehan K. Object Based Image Analysis Technique for Distinguishing Tropical Native Forest from Plantations: A Landcover Classification Analysis of Patches Surrounding the Serra do Brigadeiro State Park, Minas Gerais, Brazil. Duke University 2016.

Mishra N, Haque MO, Leigh L, Aaron D, Helder D, Markham B. Radiometric cross calibration of Landsat 8 operational land imager (OLI) and Landsat 7 enhanced thematic mapper plus (ETM+). Remote Sensing 2014; 6: 12619-12638.

Ngo QT, Dang HR. On the river bank erosion in Tan Duc, Ba Vi, Hanoi. Geology 2005; 286: 23-26

Onojeghuo AO, Blackburn GA, Wang Q, Atkinson PM, Kindred D, Miao Y. Rice crop phenology mapping at high spatial and temporal resolution using downscaled MODIS time-series. GIScience & Remote Sensing 2018 (just-accepted).

Parresol BR. Assessing tree and stand biomass: a review with examples and critical comparisons. Forest science 1999; 45: 573-593.

QĐND. Serious erosion in the Song Lo commune, Viet Tri city, Phu Tho province. QĐND 2017; https://baomoi.com/sat-lo-nghiem-trong-tai-xa-song-lo-thanh-pho-viet-tri/c/23387429.epi.

Rinaldi M. Recent channel adjustments in alluvial rivers of Tuscany, Central Italy. Earth Surface Processes and Landforms 2003; 28: 587-608.

Ryu J-H, Won J-S, Min KD. Waterline extraction from Landsat TM data in a tidal flat: a case study in Gomso Bay, Korea. Remote Sensing of Environment 2002; 83: 442-456.

Wang G, Oyana T, Zhang M, Adu-Prah S, Zeng S, Lin H, Se J. Mapping and spatial uncertainty analysis of forest vegetation carbon by combining national forest inventory data and satellite images. Forest Ecology and Management 2009; 258: 1275-1283.

Xu H. Modification of normalised difference water index (NDWI) to enhance open water features in remotely sensed imagery. International journal of remote sensing 2006; 27: 3025-3033.

Xuan PT. River bank erosion assessment in the confluence of Thao, Da, and Lo rivers. Vietnam Journal of Earth Sciences 2012; 34: 18-24.

Yamano H, Shimazaki H, Matsunaga T, Ishoda A, McClennen C, Yokoki H, Kayanne H. Evaluation of various satellite sensors for waterline extraction in a coral reef environment: Majuro Atoll, Marshall Islands. Geomorphology 2006; 82: 398-411.

Zhu X, Liu D. Improving forest aboveground biomass estimation using seasonal Landsat NDVI time-series. ISPRS Journal of Photogrammetry and Remote Sensing 2015; 102: 222-231.